Modified-Emergency Index (MEI): Advanced Criticality Metric for Autonomous Driving in Lateral Conflict

Hao Cheng[1], Yanbo Jiang[1], Qingyuan Shi[1], Qingwen Meng[1], Keyu Chen[1], Wenhao Yu[1], Jianqiang Wang[1], Sifa Zheng*[1]

***Abstract*— Effective, reliable, and efficient evaluation of autonomous driving safety performance is essential for demonstrating its trustworthiness. Criticality metrics offer an objective approach to assessing safety in autonomous driving. While existing metrics primarily focus on longitudinal conflicts, diverse lateral conflict scenarios are prevalent in urban environments. Due to their inherent design limitations, many metrics fail to accurately quantify risks in lateral conflict scenarios. This paper proposes an advanced criticality metric—*Modified-Emergency Index (MEI)*—to precisely quantify the evasive effort required in complex urban conflicts. MEI enhances the original Emergency Index (EI) by providing a more accurate estimation of the Time for Evasive Maneuver (TEM), resulting in improved risk quantification. We validate MEI using a publicly available Lateral Conflict Resolution Dataset based on Argoverse-2. From this dataset, we extract over 1,500 high-quality conflict instances involving autonomous vehicles (AVs), including 500+ critical conflicts. MEI is then compared against the well-established metric ACT and the widely used PET. Experimental results reveal multiple failure cases of ACT and PET, whereas MEI consistently shows superior performance in capturing risk trends. Overall, these findings highlight MEI as a promising metric for evaluating urban conflicts and enhancing the safety assessment framework for autonomous driving. The open-source implementation is available at `https://github.com/AutoChengh/MEI`.**

I. Introduction

Autonomous driving technology shows great potential in improving traffic safety, efficiency, and sustainability. To verify the reliability of autonomous vehicles (AVs), it is essential to establish trustworthy and effective safety performance metrics. One proactive and objective approach to evaluating AV behavioral safety is the development and use of criticality metrics. Criticality refers to “the composite risk involving all actors as the traffic situation evolves” [1]. Criticality metrics offer a surrogate way to quantify this risk from specific perspectives. Currently, they are widely applied in the field of autonomous driving, such as for safety evaluation, identifying critical events from large datasets to build scenario libraries, and supporting the development of regulatory frameworks for AVs.

Urban environments involve numerous high-risk conflicts, making them a key focus during the development of autonomous driving systems. These environments often feature various types of multi-angle conflicts, such as intersection crossing and merging/diverging situations. They also involve frequent traffic violations and complex interactions with different types of Vulnerable Road Users (VRUs). Accurately assessing the safety of AVs in urban settings is therefore a central task for criticality metrics. Most existing criticality metrics originate from Surrogate Safety Measures (SSMs) developed in the 1960s and 1970s, which were designed as proactive and efficient alternatives to crash data for road safety analysis [2]. Classic SSMs such as Time-to-Collision (TTC) remain useful for evaluating longitudinal risk, such as rear-end collisions. However, TTC is limited in capturing lateral conflicts, which are more common in urban areas. To address this, researchers have proposed metrics like Post-Encroachment Time (PET) [3] and Time Advantage (TAdv) [4]. In addition, several efforts have been made to extend TTC to account for more complex interactions in 2D space. Notable examples include Extended TTC (ETTC) [5], Anticipated Collision Time (ACT) [6], and 2D-TTC [7]. More recently, scholars have introduced the Emergency Index (EI) [8], which provides a novel approach to quantify the difficulty of evasive maneuvers. Unlike traditional metrics, EI is applicable to multi-angle conflicts. It builds on the concept of Interaction Depth (InDepth), which measures the extent of spatial intrusion between two vehicles if no evasive action is taken. A positive InDepth indicates that a collision is inevitable without avoidance. Thus, the essence of the evasive task is to reduce InDepth from positive to negative within the remaining time. EI quantifies this difficulty by defining the required rate of change of InDepth to avoid a collision. Although InDepth fully considers the geometric dimensions of the vehicles, the remaining time available for evasive action in EI is estimated using a centroid-based method. This approximation may reduce the accuracy of EI in evaluating risk in some safety-critical near-miss situations. Moreover, while several existing criticality metrics are applicable to lateral conflicts, few studies have rigorously validated their effectiveness [9]–[12]. Understanding the strengths and failure cases of different metrics is essential for establishing reliable indicators for lateral conflict evaluation.

In this paper, we propose an advanced criticality metric called the Modified-Emergency Index (MEI) to address the challenge of accurately assessing the criticality of safety-critical scenarios in urban environments. We validate MEI using an open-source lateral conflict resolution dataset based on Argoverse 2, and compare its performance with several mainstream criticality metrics, including ACT and PET. The contributions of this paper include:

This work was supported by Tsinghua-Toyota Joint Research Institute Inter-disciplinary Program.

[1]Hao Cheng, Yanbo Jiang, Qingyuan Shi, Qingwen Meng, Keyu Chen, Wenhao Yu, Jianqiang Wang, Sifa Zheng are with School of Vehicle and Mobility, Tsinghua University, Beijing 100084, P. R. China.

Corresponding author: Sifa Zheng, E-mail: zsf@tsinghua.edu.cn

1) We propose an advanced criticality metric, MEI, which improves the original Emergency Index by providing a more accurate estimation of temporal proximity. This enhancement enables a more precise evaluation of evasive effort.
2) Through experiments, we identify several failure cases of ACT and PET and conduct detailed failure analyses. We find that MEI outperforms ACT in capturing risk trends, showing its potential as a more reliable metric for evaluating the criticality of complex lateral conflicts in urban scenarios.

The rest of the paper is organized as follows. Section II introduces the computational methodology of MEI. Section III presents the validation results and failure analysis of MEI and other criticality metrics. Finally, Section IV concludes the paper.

II. Methodology

In this section, we present the computation method of the Modified-Emergency Index (MEI), including the calculation of Interaction Depth (InDepth) and Time for Evasive Maneuver (TEM). We also define formal criteria within the MEI framework to identify potential conflicts, critical conflicts, and crash moments. Following this, we describe the Lateral Conflict Resolution Dataset used in this study and the procedure for extracting high-risk cases.

A. Interaction Depth (InDepth)

We assume that the state vector of vehicle i at a given time $t \in \mathbb{R}^+$ is denoted as

$$\boldsymbol{S}_i(t) = [x_i(t),\ y_i(t),\ v_i(t),\ \theta_i(t),\ l_i,\ w_i]^T,$$

where $x_i(t)$ and $y_i(t)$ represent the X and Y coordinates of the geometric center of vehicle i, $v_i(t)$ and $\theta_i(t)$ denote its speed magnitude and heading angle, and l_i and w_i represent the length and width of the vehicle, respectively. Based on this definition, the position vector $\boldsymbol{P}_i(t)$, velocity vector $\boldsymbol{v}_i(t)$, and direction unit vector $\boldsymbol{\theta}_i(t)$ can be expressed as follows:

$$\begin{cases} \boldsymbol{P}_i(t) = \left[x_i(t),\ y_i(t)\right]^T \\ \boldsymbol{v}_i(t) = \left[v_i(t)\cos\left(\theta_i(t)\right),\ v_i(t)\sin\left(\theta_i(t)\right)\right]^T \\ \boldsymbol{\theta}_i(t) = \left[\cos\left(\theta_i(t)\right),\ \sin\left(\theta_i(t)\right)\right]^T = \dfrac{\boldsymbol{v}_i(t)}{\|\boldsymbol{v}_i(t)\|} \end{cases} \tag{1}$$

In the relative coordinate system of vehicle B, the relative position vector of vehicle A is denoted as $\boldsymbol{P}_{AB} = \left[x_A - x_B,\ y_A - y_B\right]^T$, and the relative velocity vector is computed as:

$$\boldsymbol{v}_{AB} = \boldsymbol{v}_A - \boldsymbol{v}_B = \begin{bmatrix} v_A\cos(\theta_A) - v_B\cos(\theta_B) \\ v_A\sin(\theta_A) - v_B\sin(\theta_B) \end{bmatrix} \tag{2}$$

The direction unit vector of the relative velocity is:

$$\boldsymbol{\theta}_{AB} = \frac{\boldsymbol{v}_{AB}}{\|\boldsymbol{v}_{AB}\|} \tag{3}$$

The tangential Euclidean distance between the two centers of mass D_c^T is given by:

$$D_c^T = \|\boldsymbol{P}_{AB} \times \boldsymbol{\theta}_{AB}\| \tag{4}$$

To account for vehicle size, we define the vectors from the vehicle center to the four corners of the rectangular body as:

$$\begin{cases} \overrightarrow{AA_i} = (-1)^{\lfloor i-\frac{1}{2}\rfloor}\dfrac{l_A}{2}\boldsymbol{\theta}_A + (-1)^i\dfrac{w_A}{2}\boldsymbol{\theta}_A^{\perp}, & i \in \{1,2,3,4\} \\ \overrightarrow{BB_j} = (-1)^{\lfloor j-\frac{1}{2}\rfloor}\dfrac{l_B}{2}\boldsymbol{\theta}_B + (-1)^j\dfrac{w_B}{2}\boldsymbol{\theta}_B^{\perp}, & j \in \{1,2,3,4\} \end{cases} \tag{5}$$

Here, $\boldsymbol{\theta}_A^{\perp}$ is obtained by rotating $\boldsymbol{\theta}_A$ counterclockwise by 90°, following the right-hand rule.

To fully consider vehicle size, we define the projection radii d_A and d_B as the maximum distance from the vehicle center to its body corners in the direction orthogonal to the relative velocity:

$$\begin{cases} d_A = \max\limits_{i\in\{1,2,3,4\}} \left\|\overrightarrow{AA_i} \times \boldsymbol{\theta}_{AB}\right\| \\ d_B = \max\limits_{j\in\{1,2,3,4\}} \left\|\overrightarrow{BB_j} \times \boldsymbol{\theta}_{AB}\right\| \end{cases} \tag{6}$$

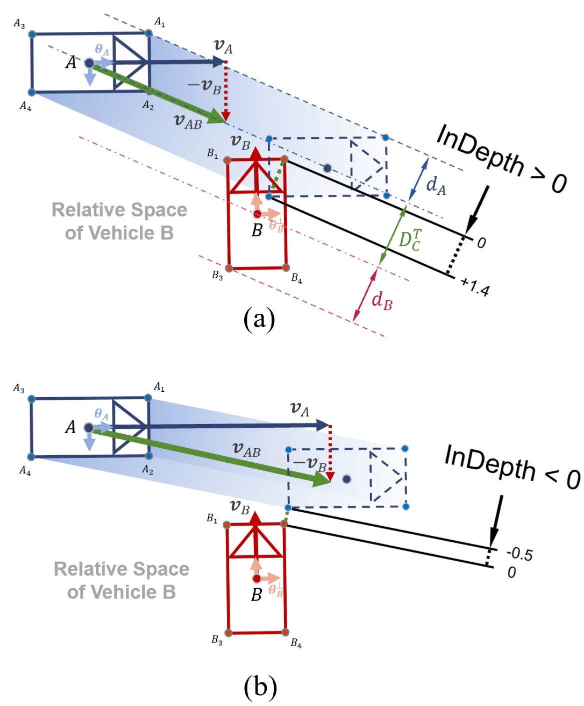

Fig. 1: Illustration of Interaction Depth (InDepth). (a) When InDepth is positive, a collision is inevitable if no evasive maneuver is taken. (b) When InDepth is negative, the two vehicles will not collide if both maintain their current motion states.

Due to vehicles' risk-sensitive nature, the space they aim to protect often extends beyond the physical body of the vehicle and may include a surrounding buffer zone [13]. We model this protected area using a safety region, as illustrated in Fig. 2 The safety region is defined as a rounded rectangle enclosing the vehicle body, with a corner radius denoted as D_{safe}. Here, D_{safe} represents the minimum inter-vehicle distance that is still considered acceptable by the vehicle.

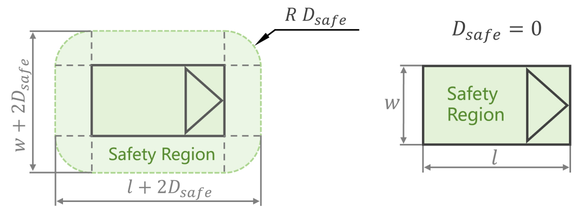

Fig. 2: Illustration of the safety region. Specifically, when $D_{\text{safe}} = 0$, the safety region is identical to the vehicle body.

Furthermore, we introduce the concept of Interaction Depth (InDepth) to quantify the maximum depth to which two vehicles may intrude into each other's safety regions in the future. The calculation is given by:

$$InDepth = d_A + d_B - D_c^T + D_{\text{safe}} \tag{7}$$

In particular, when $D_{\text{safe}} = 0$, InDepth represents the required tangential clearance between vehicles without any safety buffer. In this case, the safety region becomes identical to the vehicle body. To ensure consistency and generality, we set $D_{\text{safe}} = 0$ throughout the following analysis.

B. Modified-Emergency Index (MEI)

For two vehicles in a conflict state, a transition to a safer state requires the execution of an evasive maneuver within a limited time window, referred to as the Time for Evasive Maneuver (TEM). The necessary change for avoiding collision is measured by the Interaction Depth (InDepth). We define the Modified-Emergency Index (MEI) as the ratio between InDepth and TEM, as shown in Eq. 8. A smaller TEM or a larger InDepth results in a higher MEI, indicating that MEI is positively correlated with both the risk level and the urgency of the conflict.

$$MEI = \frac{InDepth}{TEM} \tag{8}$$

To quantify TEM, we adopt the 2D-TTC proposed by Jiao [14]. Unlike ACT, which focuses on the closest pair of points on the vehicles' bounding boxes and computes time-to-collision by projecting the relative velocity onto the direction of their closest approach, 2D-TTC evaluates the actual point pair expected to collide under a Constant Velocity (CV) model. As shown in Fig. 3, this model avoids the underestimation of collision time and overestimation of risk, making 2D-TTC a more accurate method for estimating TEM.

Furthermore, by incorporating the Conflict Detection Model (CDM) proposed by Cheng et al. [8] and setting a reasonable threshold for TEM (e.g., $\text{TEM}^* = 3\,\text{s}$), we can formally determine whether a conflict exists at any given time step, as summarized in Table I.

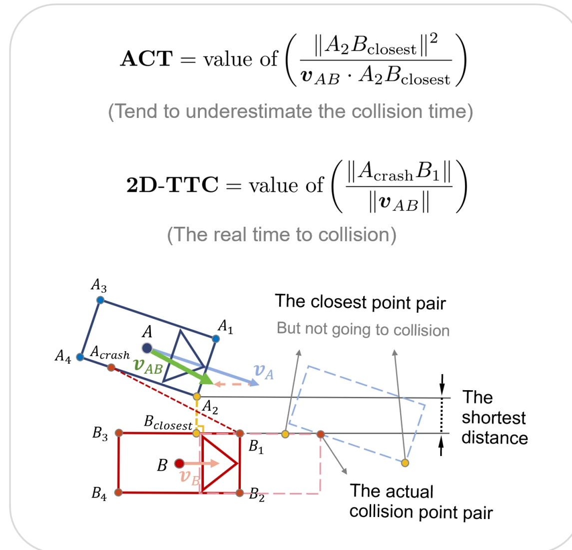

Fig. 3: Illustration of ACT and 2D-TTC calculations. In this case, the collision time estimated by ACT is approximately half of that estimated by 2D-TTC.

C. Lateral Conflict Resolution Dataset

The Argoverse-2 dataset [15] is collected by an AV fleet operating in six cities. It contains 250,000 driving scenarios, with a particular focus on safety-critical and long-tail events. Each scenario lasts for 11 seconds and is sampled at a frequency of 10 Hz. In addition, the dataset provides high-definition map information, including vectorized lane maps and drivable area annotations. Based on the Argoverse-2 dataset, Li et al. [16] construct and release a high-quality lateral conflict resolution dataset[1]. This dataset is developed through a rigorous data processing pipeline that includes anomaly correction and ensures balanced traffic conditions across various conflict types.

Based on the lateral conflict resolution dataset, we use the Separating Axis Theorem (SAT) [17] to filter out collision cases. After processing, we obtain 1,548 conflict instances with a maximum MEI greater than zero, in which the AV is involved as one of the risk participants. According to the formal criteria listed in Table I, 501 of these cases are classified as critical conflicts (32.4%), while the remaining 1,047 are identified as potential conflicts (67.6%).

III. Results

In this section, we analyze high-risk AV cases based on the lateral conflict resolution dataset introduced in Section II. We employ the MEI along with widely used criticality metrics, including the ACT and the PET. Statistical results are presented first, followed by case studies that highlight the advantages of MEI.

[1] https://github.com/RomainLITUD/conflict_resolution_dataset

TABLE I: The MEI framework for judging potential conflict, critical conflict, and crash moment

	Non-Conflict	Potential Conflict	Critical Conflict	Crash
Condition Q in CDM [8]	$\times$	✓	✓	✓
TEM (s)	-	-	$\leq$ TEM*	$\rightarrow 0$
InDepth (m)	-	-	≥ 0	$\geq D_{\text{safe}}$
MEI (m/s)	-	-	≥ 0	$\rightarrow +\infty$

A. Statistical Analysis of AV Conflicts Using Criticality Metrics

To further investigate the risk distribution of AV-involved conflict events, we compute the maximum MEI, the minimum ACT, and the PET for each of the 1,548 conflict samples. The distributions of these criticality metrics are illustrated in Fig. 4. Furthermore, Table II summarizes the risk-level thresholds based on percentile rankings. These statistical results provide a foundation for stratifying conflict severity and support the establishment of evaluation benchmarks for identifying critical events. In the following analysis, we identify potential failure cases by examining instances where the risk levels differ significantly across different criticality metrics.

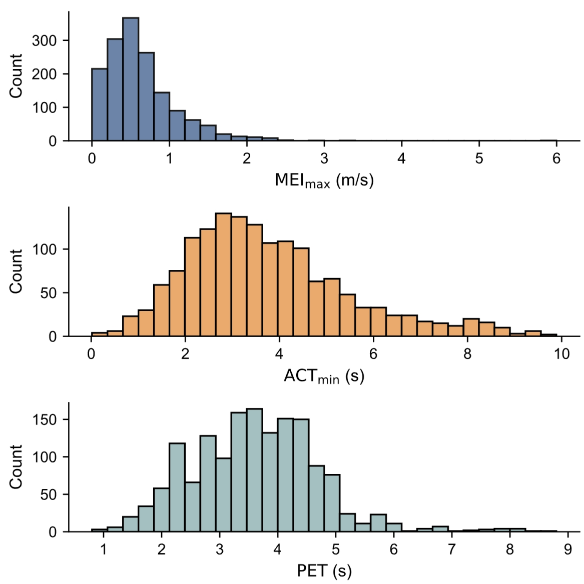

Fig. 4: Distributions of criticality metrics: (top) MEI$_{\text{max}}$, (middle) ACT$_{\text{min}}$, and (bottom) PET.

B. Failure Case Analysis

*1) **Case 1: False Alarm (False Positive) by ACT**:* As shown in Fig. 5, this case involves a lateral conflict where the AV turns right at an intersection and encounters a pedestrian approaching from the right. Throughout the scenario, the PET is 2.4 s. In this case, the maximum MEI is 0.35 m/s (occurring at $t = 0.1$ s), indicating that the situation is a manageable safety-critical event. However, ACT suggests the event is highly risky, with a minimum value of 0.60 s at $t = 3.5$ s. Further analysis reveals that at $t = 3.5$ s, the AV is about to exit the conflict zone, while the pedestrian is preparing to

TABLE II: Risk-level thresholds for MEI$_{\text{max}}$, ACT$_{\text{min}}$, and PET

Risk Level	**MEI$_{\text{max}}$ (m/s)**	**ACT$_{\text{min}}$ (s)**	**PET (s)**
Top 1%	**2.13** (99th)	**0.77** (1st)	**1.40** (1st)
Top 5%	**1.52** (95th)	**1.43** (5th)	**2.00** (5th)
Top 10%	**1.22** (90th)	**1.85** (10th)	**2.20** (10th)
Top 25%	**0.81** (75th)	**2.52** (25th)	**2.80** (25th)
Top 50%	0.53 (50th)	3.47 (50th)	3.60 (50th)
Top 75%	0.33 (25th)	4.66 (75th)	4.30 (75th)
Top 90%	0.14 (10th)	6.19 (90th)	4.80 (90th)
Top 95%	0.08 (5th)	7.43 (95th)	5.30 (95th)
Top 99%	0.01 (1st)	8.78 (99th)	6.95 (99th)

pass behind the AV from the right rear. Although the TEM is only 0.60 s, the *InDepth* is merely 0.0014 m, resulting in an MEI of just 0.0024 m/s—indicating low actual evasive difficulty.

*2) **Case 2: Missed Detection by PET**:* As shown in Fig. 6, Case 2 involves a lateral conflict where the AV proceeds straight through an intersection and encounters an Human-driven Vehicle (HV) approaching from the right. The maximum MEI is 0.81 m/s (occurring at $t = 0.4$ s), and the minimum ACT is 1.22 s (at $t = 0.6$ s), both indicating a safety-critical event. However, at $t = 2.2$ s, after the AV has passed through the intersection, the HV does not proceed immediately but instead enters the potential conflict zone at $t = 10.4$ s. This results in a PET value of 8.2 s, which suggests a non-conflict or only a potential conflict. The delayed entry of the HV may be due to a traffic signal or an unexpected situation (the dataset does not specify the cause). As a result, PET appears to underestimate the actual risk in this case.

*3) **Case 3: False Alarm (False Positive) by PET**:* As shown in Fig. 7, Case 3 involves a lateral conflict where the AV proceeds straight and encounters a pedestrian crossing the road from the left. In this case, the maximum MEI is 0.32 m/s (at $t = 0.2$ s), and the minimum ACT is 2.99 s (at $t = 1.3$ s), both indicating a low and manageable risk. However, after the AV exits the conflict zone at $t = 4.3$ s, the pedestrian enters the zone at $t = 5.2$ s, resulting in a PET of only 0.9 s—classified as high risk under PET's threshold-based system. Further analysis reveals that the pedestrian enters the conflict zone only after the AV has already passed through, and maintains a constant speed throughout the interaction. Therefore, there is no significant risk following the AV's passage, and PET tends to overestimate the actual risk in this

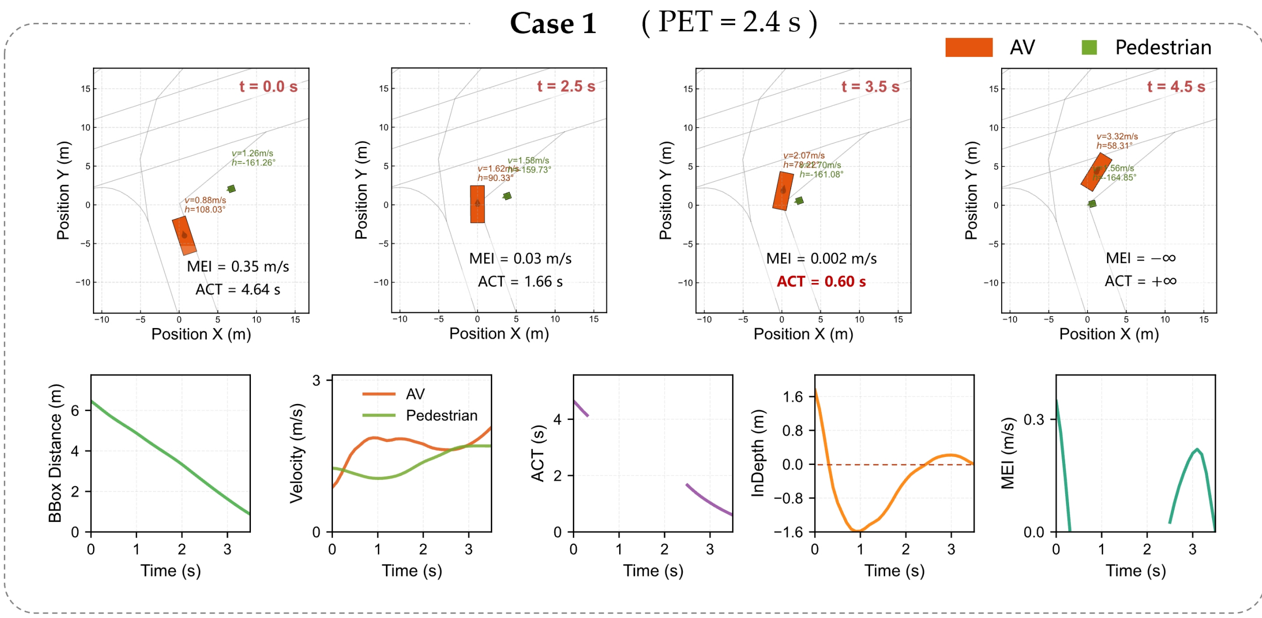

Fig. 5: A lateral conflict scenario where the AV turns right and a pedestrian approaches from the right. The minimum ACT is $0.60\,\mathrm{s}$, indicating that ACT may overestimate the actual risk.

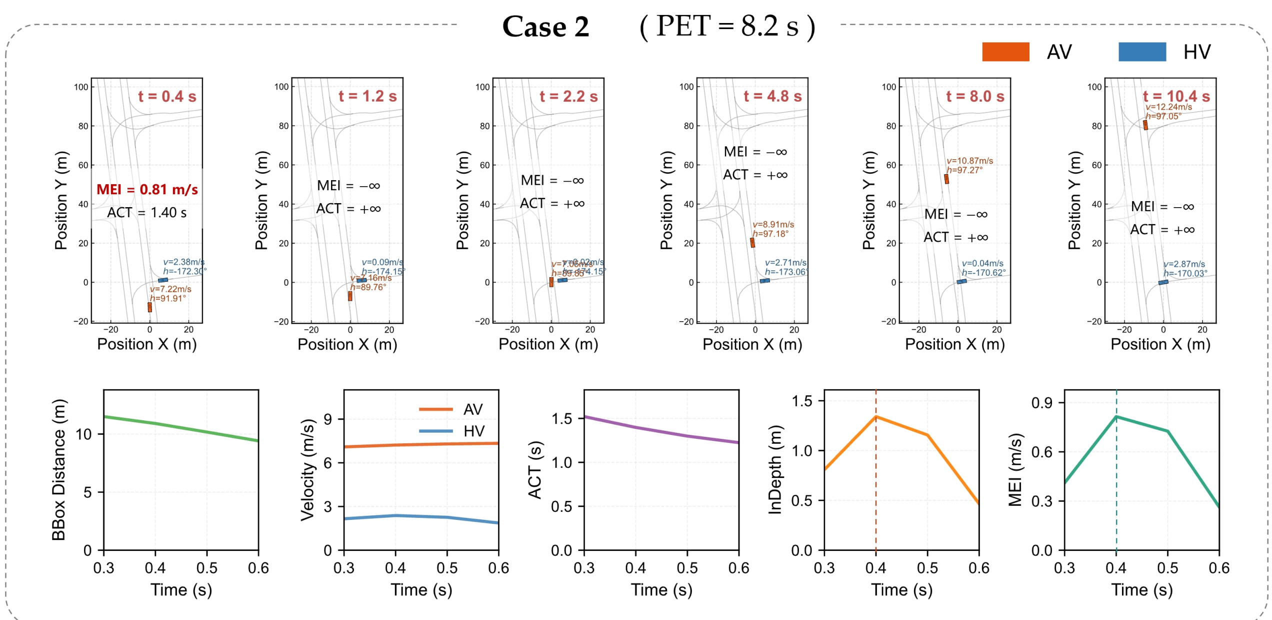

Fig. 6: A lateral conflict where the AV proceeds straight through an intersection and encounters an HV from the right. Although the PET is $8.2\,\mathrm{s}$, both ACT and MEI indicate a safety-critical event, suggesting that PET may underestimate the actual risk.

case.

Cases 2 and 3 collectively indicate that PET's risk quantification is strongly influenced by the behavior of the second road user. When the critical interaction primarily occurs during the lead vehicle's traversal, PET may not reliably capture the actual level of risk.

*4) **Case 4: High-Risk Near-Miss Scenario**:* As shown in Fig. 8, Case 4 involves a lateral conflict in which the AV makes a left turn at an intersection and encounters a straight-moving HV. In this case, PET is $2.4\,\mathrm{s}$. The maximum MEI is $3.21\,\mathrm{m/s}$ (at $t = 5.4\,\mathrm{s}$), and the minimum ACT is $0.75\,\mathrm{s}$ (at $t = 5.9\,\mathrm{s}$), both indicating a high-risk safety-critical event. The risk arises from the HV accelerating between $t = 4.6\,\mathrm{s}$ and $t = 5.2\,\mathrm{s}$ to compete for the right-of-way with the AV, then decelerating after $t = 5.2\,\mathrm{s}$ upon yielding to the AV. From the ACT perspective, the value decreases continuously from $2.20\,\mathrm{s}$ to $0.75\,\mathrm{s}$ between $t = 4.6\,\mathrm{s}$ and $5.9\,\mathrm{s}$, suggesting steadily increasing risk. In contrast, MEI

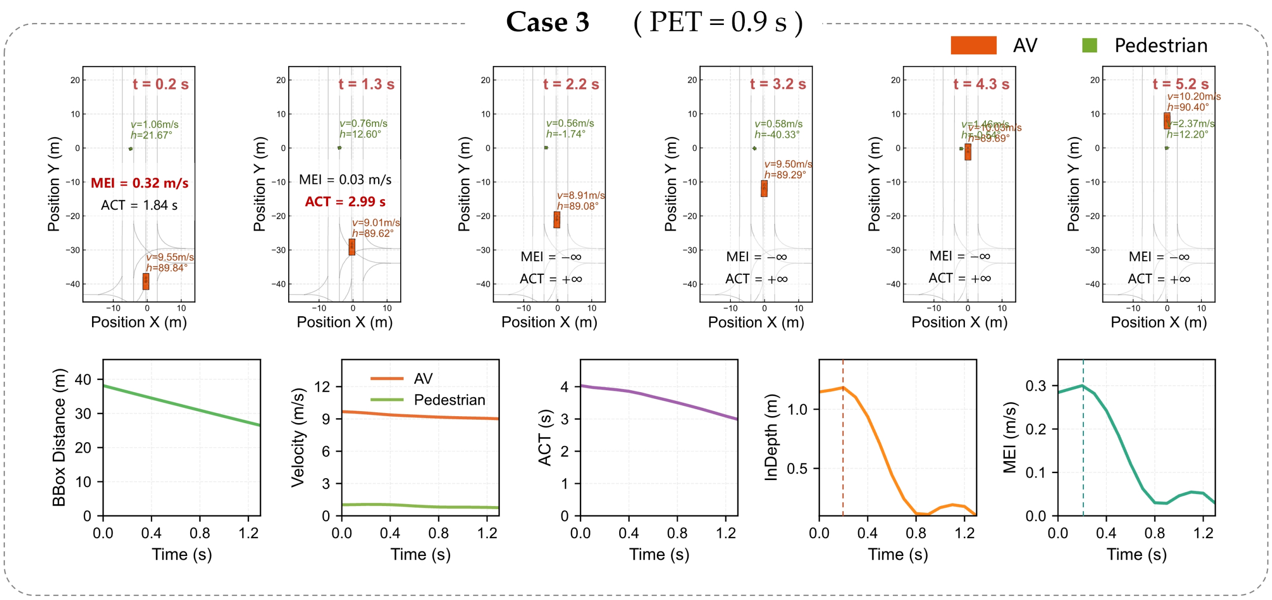

Fig. 7: A lateral conflict where the AV proceeds straight and encounters a pedestrian crossing from the left. The PET is 0.9 s, but ACT and MEI indicate low and manageable risk, suggesting that PET may overestimate the actual risk.

captures a rise-and-fall trend in risk that aligns with the HV's acceleration followed by deceleration. This suggests that MEI can provide a more precise assessment of evolving risk than ACT, offering better frame-level responsiveness. This highlights MEI's potential for deployment in real-time risk monitoring and vehicle warning systems, enabling earlier and more precise detection.

IV. Conclusions

This paper proposes an advanced criticality metric, the Modified-Emergency Index (MEI), to address the challenge of accurately assessing criticality in urban lateral conflict scenarios. We validate MEI using a lateral conflict resolution dataset based on the Argoverse-2 dataset and compare it with several mainstream criticality metrics. Experimental results show multiple failure cases of ACT and PET, while MEI consistently demonstrates accurate risk representation. These findings help reveal the limitations of widely used metrics such as ACT and PET in evaluating criticality in urban safety-critical scenarios. In a high-risk near-miss case, MEI also outperforms ACT in capturing the risk trend, suggesting that MEI has strong potential to serve as a reliable metric for assessing criticality in complex lateral conflicts in urban settings.

This study also has some limitations. It focuses on safety analysis—specifically criticality—which is a primary concern in academic research. However, a comprehensive evaluation of autonomous driving should consider safety, efficiency, and comfort. Such integrated assessment is beyond the scope of this paper and can be explored in future research. In addition, this paper only validates MEI in urban lateral conflict scenarios. Future studies may extend the analysis to highway settings to further evaluate the effectiveness and robustness of MEI.

References

[1] L. Westhofen, C. Neurohr, T. Koopmann, M. Butz, B. Schütt, F. Utesch, B. Neurohr, C. Gutenkunst, and E. Böde, "Criticality metrics for automated driving: A review and suitability analysis of the state of the art," *Archives of Computational Methods in Engineering*, vol. 30, no. 1, pp. 1–35, 2023.

[2] P. Tafidis and A. Pirdavani, "Application of surrogate safety measures in higher levels of automated vehicles simulation studies: A review of the state of the practice," *Traffic injury prevention*, vol. 24, no. 3, pp. 279–286, 2023.

[3] B. L. Allen, B. T. Shin, and P. J. Cooper, "Analysis of traffic conflicts and collisions," Tech. Rep., 1978.

[4] A. Laureshyn, Å. Svensson, and C. Hydén, "Evaluation of traffic safety, based on micro-level behavioural data: Theoretical framework and first implementation," *Accident Analysis & Prevention*, vol. 42, no. 6, pp. 1637–1646, 2010.

[5] J. R. Ward, G. Agamennoni, S. Worrall, A. Bender, and E. Nebot, "Extending time to collision for probabilistic reasoning in general traffic scenarios," *Transportation Research Part C: Emerging Technologies*, vol. 51, pp. 66–82, 2015.

[6] S. P. Venthuruthiyil and M. Chunchu, "Anticipated collision time (act): A two-dimensional surrogate safety indicator for trajectory-based proactive safety assessment," *Transportation research part C: emerging technologies*, vol. 139, p. 103655, 2022.

[7] H. Guo, K. Xie, and M. Keyvan-Ekbatani, "Modeling driver's evasive behavior during safety–critical lane changes: Two-dimensional time-to-collision and deep reinforcement learning," *Accident Analysis & Prevention*, vol. 186, p. 107063, 2023.

[8] H. Cheng, Y. Jiang, H. Zhang, K. Chen, H. Huang, S. Xu, J. Wang, and S. Zheng, "Emergency index (ei): A two-dimensional surrogate safety measure considering vehicles' interaction depth," *Transportation Research Part C: Emerging Technologies*, vol. 171, p. 104981, 2025.

[9] K. Ismail, T. Sayed, and N. Saunier, "Methodologies for aggregating indicators of traffic conflict," *Transportation research record*, vol. 2237, no. 1, pp. 10–19, 2011.

[10] K. Salamati, B. Schroeder, N. M. Rouphail, C. Cunningham, R. Long, and J. Barlow, "Development and implementation of conflict-based assessment of pedestrian safety to evaluate accessibility of complex intersections," *Transportation research record*, vol. 2264, no. 1, pp. 148–155, 2011.

[11] A. Arun, M. M. Haque, A. Bhaskar, S. Washington, and T. Sayed, "A systematic mapping review of surrogate safety assessment using traffic conflict techniques," *Accident Analysis & Prevention*, vol. 153, p. 106016, 2021.

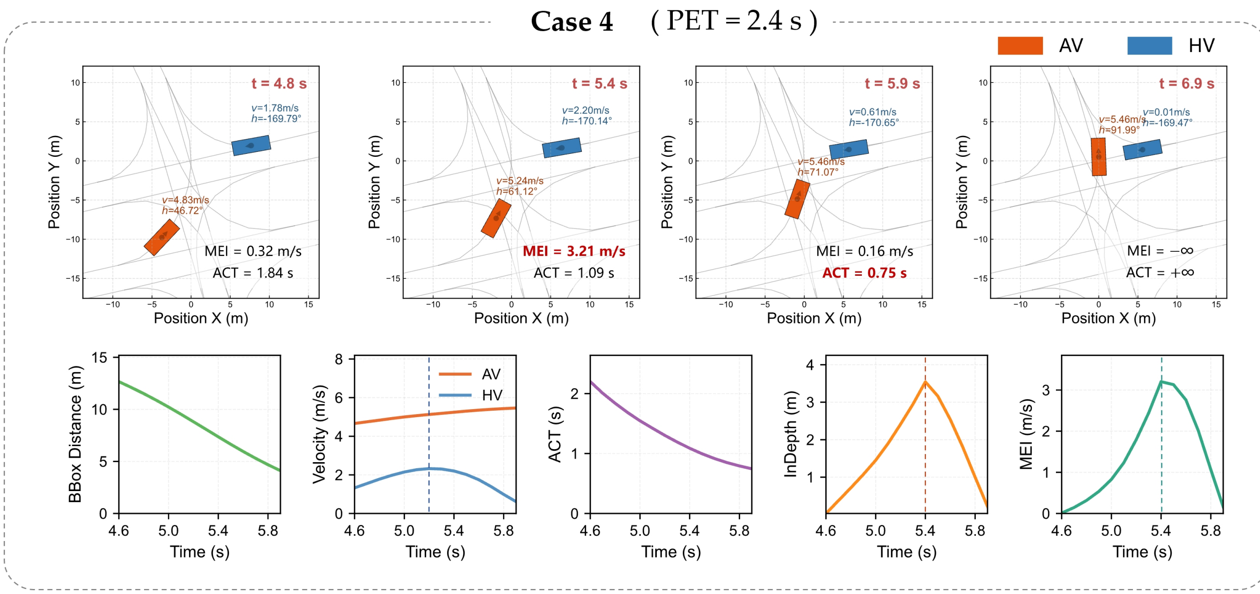

Fig. 8: A lateral conflict where the AV turns left and encounters a straight-driving HV. MEI's risk assessment aligns with vehicle behavior, suggesting higher frame-level accuracy.

[12] Y. Jiao, S. C. Calvert, S. van Cranenburgh, and H. van Lint, "A unified probabilistic approach to traffic conflict detection," *Analytic Methods in Accident Research*, vol. 45, p. 100369, 2025.

[13] J. Hou, G. F. List, and X. Guo, "New algorithms for computing the time-to-collision in freeway traffic simulation models," *Computational intelligence and neuroscience*, vol. 2014, no. 1, p. 761047, 2014.

[14] Y. Jiao, "A fast calculation of two-dimensional Time-to-Collision," Mar. 2023. [Online]. Available: https://github.com/Yiru-Jiao/Two-Dimensional-Time-To-Collision

[15] B. Wilson, W. Qi, T. Agarwal, J. Lambert, J. Singh, S. Khandelwal, B. Pan, R. Kumar, A. Hartnett, J. K. Pontes, *et al.*, "Argoverse 2: Next generation datasets for self-driving perception and forecasting," *arXiv preprint arXiv:2301.00493*, 2023.

[16] G. Li, Y. Jiao, S. C. Calvert, and J. H. van Lint, "Lateral conflict resolution data derived from argoverse-2: Analysing safety and efficiency impacts of autonomous vehicles at intersections," *Transportation Research Part C: Emerging Technologies*, vol. 167, p. 104802, 2024.

[17] S. Gottschalk, "Separating axis theorem," 1996.